Water Resour Manage (2010) 24:2247–2266
DOI 10.1007/s11269-009-9550-y

Spatial Distributions of Soil Surface-Layer Saturated Hydraulic Conductivity and Controlling Factors on Dam Farmlands

Peipei Zhao · Mingan Shao · Tiejun Wang

Received: 6 January 2009 / Accepted: 6 December 2009 /
Published online: 30 December 2009

Abstract Saturated hydraulic conductivity (*Ks*) is a critical soil property affecting water flow and solute transport. In the Loess Plateau of China, sloping farmlands have been increasingly replaced by dam farmlands to achieve higher crop yields and more importantly to control soil erosions. It is necessary to understand the spatial pattern of near-surface K_S on those newly formed dam farmlands, because the land surface processes (e.g., erosion that is controlled by overland flow) are largely determined by the spatial distribution of near-surface *Ks*. In this study, near-surface *Ks* (e.g., 5 cm depth of the surface layers) was measured using 336 undisturbed soil samples collected from two dam farmlands located in the Liudaogou catchment, a heavily studied catchment in the Loess Plateau of China. Based on classical and geostatistical analyses, the soil properties at the filled dam farmland showed more spatial variations compared to the silting dam farmland. Statistical scale-invariance was evaluated using the Hurst scaling parameter (*H*) for different soil parameters. The *H* values ranged from 0.646 to 0.877, indicating certain degrees of statistical scale-invariance and long-range dependency within the spatial range. The bulk density (D_b), saturated water content (SW), sand content (SA), silt content (SI), and clay content (CL) were shown to affect the K_S values significantly with SW, SI, and CL negatively and SA and D_b positively correlated with K_S. The highest

P. Zhao
State Key Laboratory of Soil Erosion and Dryland Farming on the Loess Plateau,
Institute of Soil and Water Conservation,
CAS & MWR, Yangling, China

M. Shao (✉)
State Key Laboratory of Soil Erosion and Dryland Farming on the Loess Plateau,
Institute of Soil and Water Conservation,
Northwest A&F University, Yangling, China
e-mail: mashao@ms.iswc.ac.cn

T. Wang
School of Natural Resources, University of Nebraska-Lincoln,
521 Hardin Hall, Lincoln, NE 68583, USA

K_S value was found at the middle portion of the dam farmlands and the lowest value was found at the locations with the minimum occurrence of surface runoff. In addition, the areas with lowest K_S values corresponded to the areas with the highest CL, SI, and SW. The results showed that disturbing soil structure by planting crops would benefit the floodwater control on dam farmlands due to increased Ks and the flooding on dam farmlands would be eased due to the silting process.

Keywords Dam farmland · Saturated hydraulic conductivity · Surface-layer · Spatial distribution · Contributing factors

1 Introduction

Soil saturated hydraulic conductivity (K_S) is a critical property affecting water flow and solute transport in soils, and consequently influencing soil evaporation and groundwater recharge under natural conditions and in agricultural fields (De Vries and Simmers 2002; Rai et al. 1998; Wang et al. 2009a, b, c). In undulating regions like the Loess Plateau of China with high hillslopes, knowledge of K_S and its spatial distribution in topsoils is of particular importance, as near-surface K_S largely determines the partitioning of precipitation into infiltration and surface runoff (e.g., infiltration excess overland flow), which in turn impacts sediment transport capacity and erosion rate (Shi and Shao 2000; Burt 2001). Due to the lack of vegetation cover and impropriate land use, the Loess Plateau of China with an area over 624,000 km^2 has experienced exceptionally high soil erosion rates compared to other regions in the world. The average erosion rate in this region is approximately 150 Mg ha^{-1} year^{-1} and the maximum rate may reach as high as 390 Mg ha^{-1} year^{-1} (Chen and Luck 1989). Despite the significant impact of near-surface K_S on land surface processes, the spatial distribution of K_S has been rarely investigated in the Loess Plateau of China.

To protect the landscapes in the Loess Plateau of China from soil erosions, a number of measures have been implemented (e.g., artificial forestation), among which check-dams are considered to be a very promising one (Gao and Zhang 2007). Check-dams are barriers built across rivers or streams, which are used to control soil and water losses and to form dam farmlands in the region (Gao and Zhang 2007). Dam farmlands, which are formed by the intercepted sediments, provide critical agricultural opportunities for the local farmers in terms of crop productions, as the crop yield of dam farmlands is usually 4–6 times higher than the one of sloping farmlands, sometimes even exceeding 10 times (Xu and Wang 2000). As such, check-dams have been widely used as a conservative practice in the region to control soil erosion and water loss as well as to maintain sustainable developments for local economies. By 2003, there were about 113,500 check-dams, which formed 3,340 km^2 dam farmland, held 2.1 $\times$ 10^{10} m^3 of sediments, and controlled 9,247 km^2 drainage area in the Loess Plateau of China. The number of check-dams and the area of dam farmlands are expected to double by 2020 (Gao and Zhang 2007). However, constant floods have caused some of the dam farmlands not suitable for agricultural purposes due to anaerobic conditions in the soil (Zhang et al. 2007), which in turn are impacted by the spatial distributions of near-surface K_S on dam farmlands (e.g., infiltration). Because of the hydrological, geomorphological, and economic importance of the

dam farmlands, it is prerequisite to understanding the spatial pattern of near-surface K_S distributions and particularly its interactions with controlling factors (e.g., soil texture and porosity) on those farmlands.

Recent studies (Sobieraj et al. 2004; Zeleke and Si 2005) showed that geostatistical methods are useful tools for characterizing the spatial pattern of K_S and for determining the degree of its cross-correlation with other soil properties. Sobieraj et al. (2004) investigated the spatial distributions of K_S and tested the hypothesis that whether structural variance emerges from noise with increasing sampling precision. Zeleke and Si (2005) examined the variability in K_S at observational scales and its relationships with other soil properties using geostatistical methods. However, to our best knowledge, geostatistical methods have never been used to characterize the spatial dependency of K_S on soil properties on newly formed dam farmlands.

In this study, our objectives were: (1) to measure K_S in topsoils at two small dam farmlands as well as other soil properties, including bulk density (D_b), saturated water content (SW), and contents of sand (SA), silt (SI), and clay (CL); (2) to investigate the spatial distributions of K_S; and (3) to evaluate the spatial dependency of K_S on the spatial patterns of its controlling factors using both classical and geostatistical techniques.

2 Study Site and Methodology

2.1 Study Area

The study site is located at the Liudaogou catchment in the northwestern Shaanxi province, China. The drainage area of the catchment is 6.9 km^2 with the mean ravine density of 7.4 km/km^2. At the site, the mean annual precipitation is approximately 437.4 mm/year, most of which is received from June to September, and the mean potential evapotranspiration is 1,336.6 mm/year. The mean aridity index (i.e., the ratio of mean potential evapotranspiration to precipitation) is 3.1. The mean annual temperature is 8.4°C The catchment falls in the center of the Water–wind erosion crisscross region, where very serious soil erosion occurs. The mean soil erosion modulus is 150 Mg ha^{-1} $year^{-1}$ (Tang et al. 1993). The soil at the site is classified as Ust-Sandic Entisols with sandy loam textured (Hu et al. 2008).

2.2 Methodology

Two dam farmlands were selected from the Liudaogou catchment in this study (Fig. 1). No tillage practices occurred on the two dam farmlands, both of which have been silting under nature conditions since the constructions of the check dams. For the purpose of convenience, the first dam farmland is called D1, which was filled up by sediment and covered by vegetation, such as *Setaria viridis* L. and *Artemisia desterorum* S. The other farmland, which is called D2 in this study, was built in 2006 with very little vegetation covers and has only functioned for about 1 year before our field campaign.

K_S sampling points were derived from 3 × 3 m grids (Fig. 2). At each grid, an undisturbed soil sample was taken from the top 5 cm of soils in April 2008 (no silting process) using a cylindrical metal core with a height of 5 cm and a volume of 100 cm^3. Total 336 undisturbed soil samples, including 216 from D1 and 120 from D2, were collected for determining K_S and measuring other basic soil physical properties

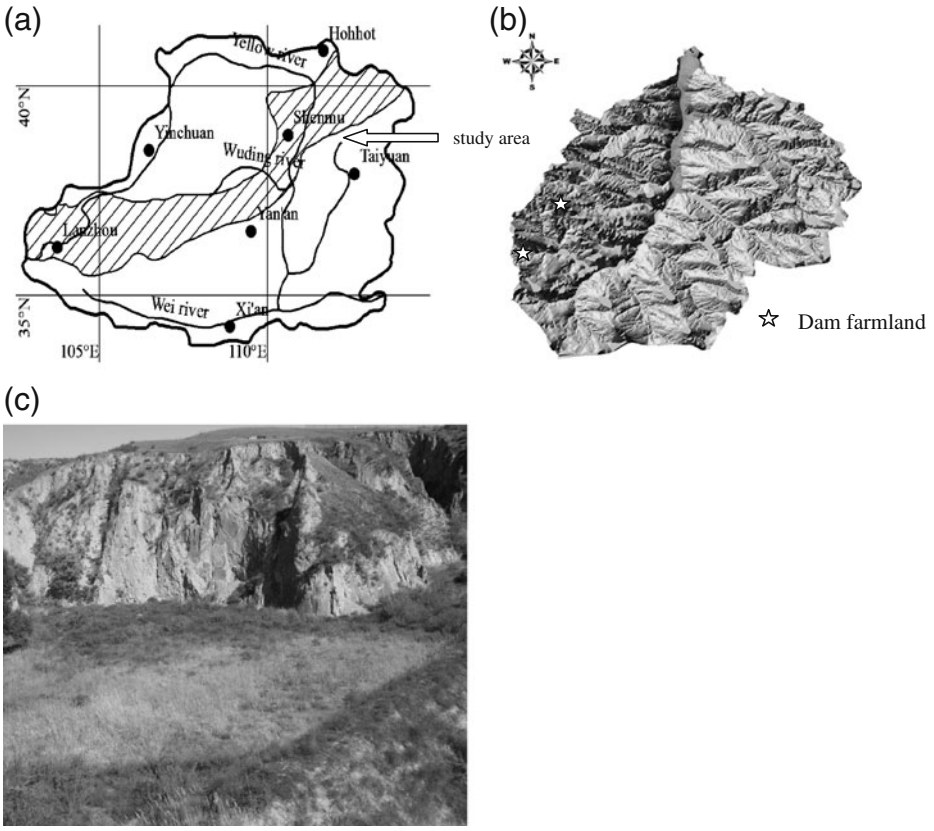

Fig. 1 The location of study area on the Loess Plateau of China, the digital elevation model of Liudaogou catchment, and the general view of filled dam farmland

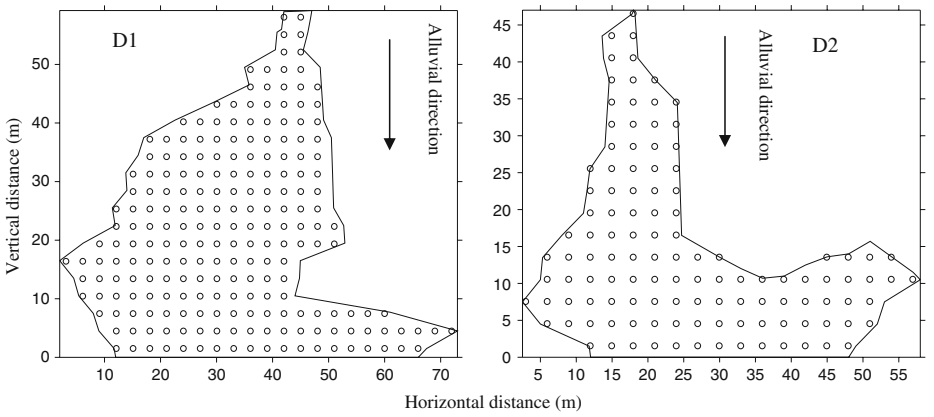

Fig. 2 Sample outline of two dam farmlands (filled dam farmland (D1), silting dam farmland (D2))

(Fig. 2). The saturated hydraulic conductivity was first measured and then the same soil sample was used to measure other basic soil physical properties. Bulk density of each soil sample was determined using the volume-mass relationship. The soil particle size distribution was determined by the method of Kettler et al. (2001).

Classical and geostatistical methods were used for the data analysis to characterize the spatial distributions of soil properties on the dam farmlands. The classical or descriptive statistical methods used in this study include mean, standard deviation (Std), coefficient of variation (CV), and skewness. The relationships of K_S with other soil parameters were determined using the Pearson correlation analysis. CV can be used to describe the magnitude of the spatial variability as low when $CV \leq 10\%$, moderate if $10\% < CV < 100\%$, and high when $CV \geq 100\%$ (Nielsen and Bouma 1985). Normality was also assessed using the one-sample Kolmogorov–Smirnov (K–S) test for determining whether a ln transformation of the dataset is necessary during the geostatistical analysis. Based on the regionalized variables theory and the intrinsic hypothesis, a semivariogram, $\gamma(h)$, can be expressed as:

$$\gamma(h) = \frac{1}{2N(h)} \sum_{i=1}^{N(h)} \left[z(x_i) - z(x_i + h) \right]^2 \tag{1}$$

where $N(h)$ is the number of pairs of observations $[z(x_i); z(x_{i+h})]$ separated by a distance h (Grego et al. 2006). The software GS + (Gamma Design Software, LLC) was employed to fit the semivariance. The geostatistical parameters, including nugget variance (C_0) that occurs at distances smaller than the sampling interval (e.g., 3 m in this study), structural variance C_1, sill variance ($C_0 + C_1$) that is the total variance, and correlation length (R) can be derived from the fitted semivariograms.

The models used for the theoretical semivariograms were the Spherical, Gaussian, and Exponential models with a nugget effect, which can be written as:

Spherical model

$$\gamma(h) = C_0 + C_1 \left[3/2\,(h/a) - 1/2\,(h/a)^3 \right] \quad 0 \leq h \leq a \tag{2a}$$

$$\gamma(h) = C_0 + C_1 \quad h > a \tag{2b}$$

Gaussian model

$$\gamma(h) = C_0 + C_1 \left(1 - \exp\left(h^2/a^2 \right) \right) \tag{3}$$

Exponential model

$$\gamma(h) = C_0 + C_1 \left(1 - e^{-h/a} \right) \quad 0 \leq h \leq a \tag{4a}$$

$$\gamma(h) = C_0 + C_1 \quad h > a \tag{4b}$$

The degree of spatial dependence (GD) was calculated as:

$$GD = C_0 / (C_0 + C_1) \tag{5}$$

The GD can be used to classify the spatial dependence as strong if GD is equal or less than 0.25, moderate if $0.25 <$ GD and is equal or less than 0.75, and weak if $GD >$ 0.75 (Cambardella et al. 1994).

A more general and well-established method to evaluate scale invariance and persistency in spatial series is through the use of scaling parameters, such as the Hurst

parameter, H (Braun et al. 1997; Pardini 2003; Zhou et al. 2004). For a self-similar as well as spatially persistent series, the value of 'spike' patterns proliferate in the scatter and the persistency of the series is reduced to verify whether the value of H significantly deviates from the interval (0.5, 1). The standard method for calculating the H parameter is given as follows (Teverovsky and Taqqu 1997; Lee 2002). An aggregated series of order m is first obtained by dividing the original series $Z(x)$ into m blocks and averaging over each block.

$$\overline{Z}(x)_{m,k} = \frac{1}{m} \sum_{i=(k-1)m+1}^{km} Z(x_i), k = 1, 2 \cdots n/m \tag{6}$$

where k labels the block and n is the total number of observations. The sample variance of the aggregated series, $\lambda(m)$, is then calculated as:

$$\lambda(m) = \frac{1}{n/m} \sum_{k=1}^{n/m} \left[Z(x)_{m,k} \right]^2 - \left[\frac{1}{n/m} \sum_{k=1}^{n/m} Z(x)_{m,k} \right]^2 \tag{7}$$

The same procedure is repeated for different m values, and then the logarithm of $\lambda(m)$ is plotted against Log(m). If the series is self-similar, the resulting points should form a straight line with a slope ζ, and furthermore, if the series is both self similar and spatially persistent (i.e., the series has a long range memory of the pattern), the slope ζ varies between -1 and 0. In practice, the slope ζ is estimated by fitting a line to the points obtained from the plot and related to H as follows (Teverovsky and Taqqu 1997).

$$H = 0.5\zeta + 1 \tag{8}$$

3 Results and Discussions

3.1 Classical and Geostatistical Analysis

Summary of classical statistics on all the soil parameters is reported in Table 1. Compared to D1, the mean values of D_b, SA, and CL of D2 are significantly larger; whereas, the mean values of SI, SW, and K_S of D2 are significantly lower (significant at $P = 0.01$). Although there are high values of D_b and SA in the D2 dataset, the values of K_S are essentially lower than the ones of D1, probably due to the relatively high contents of CL and less disturb for the young silting period. Blanco-Canqui et al. (2002) reported that fine particles usually enhance soil swelling and thus clog macropores, which results in reduced K_S values. The spatial distributions of D_b and SW are relatively uniform, with CV of 7.54% and 10.43% on D1, and 3.66% and 6.36% on D2, respectively. They belong to low spatial variability. The variability in K_S on D1 and D2 is comparable (CV of 38.29% and 37.83%, respectively), which belongs to moderate variability. The highest variability is found for CL of D1 with CV of 117.58%. Compared with other variables, the CV of CL also has the highest value on D2. The high variability in CL on both D1 and D2 are mainly caused by the low contents of CL for it would raise the effect of test error on the results. The variability in SA and SI is lower compared with CL, mainly because of the high contents of SA and SI as well as easier detachment processes, especially for SA. Generally, the CV

Table 1 Descriptive statistical test results for mean, standard deviation, variability, and data distribution with saturated hydraulic conductivity

	Mean		Std		CV (%)		Skewness[a]		K–S max (D)[b]	
	D1	D2	D1	D2	D1	D2	D1	D2	D1	D2
D_b (g/cm3)	1.38*	1.54	0.10	0.06	7.54	3.66	0.136	−0.372	0.050	0.067
SA (%)	61.75	71.67	20.15	10.37	32.64	14.47	−1.171*	−1.982*	0.128*	0.179*
Ln (SA)	4.02	4.26	0.57	0.18	14.18	4.26	−0.80	−0.77	0.051	0.062
SI (%)	34.51	26.24	17.48	9.63	50.27	36.71	0.952*	1.780*	0.117*	0.164*
Ln (SI)	3.43	3.22	0.52	0.31	15.16	9.63	−0.72	0.90	0.017	0.028
CL (%)	1.74	2.33	0.25	1.35	117.58	57.98	3.395*	2.855*	0.278*	0.182*
Ln (CL)	0.88	0.73	0.85	0.44	96.59	60.0	0.59	0.39	0.009	0.030
SW (%)	45.94	39.92	4.79	1.87	10.43	6.36	0.081	0.007	0.048	0.058
Ks (cm/min)	0.29	0.22	0.11	0.08	38.29	37.83	0.331	0.174	0.048	0.077

D_b bulk density; *SA* sand content; *SI* silt content; *CL* clay content; *SW* saturated water content; *Ks* saturated hydraulic conductivity; *Std* standard deviation; *CV* coefficient of determination, *K–S* Kolmogorov–Smirnov

[a]The critical skewness value is given by $2 \times (6/n)^{0.5}$ where n is the number of observations (Tabachnick and Fidell 1996)

[b]The critical departure value from Gaussian distribution in K–S test is given by $(1.36/n)^{0.5}$ (Massey 1951)

*$P < 0.01$

values of all the properties on D2 are lower than those of D1 (Table 1). This can be partly explained by the smaller sample size of D2 (120) than D1 (216).

The distributions of all the data were evaluated by a skewness function and tested for significance using the method suggested by Tabachnick and Fidell (1996). The critical skewness values for 216 and 120 observations are 0.333 and 0.447, respectively. The skewness in D_b, SW, and K_S (Table 1 and Fig. 3) are not significant and therefore a ln transformation of the data is not necessary. The distribution of SA is negatively skewed with the skewness values of −1.171 on D1 and −1.982 on D2. The distributions of SI and CL are positively skewed with the skewness values of 0.952 on D1 and 1.780 on D2 for SI, and 3.395 on D1 and 2.855 on D2 for CL, respectively (significant at $P = 0.01$). The normality of the data is evaluated by the K–S goodness-of-fit test and the level of significance is calculated using the method discussed by Massey (1951) (Table 1). The K–S test shows that the distributions of SA, SI, and CL are significantly different from normal distributions. The observed high skewness of SA, SI, and CL may be the result of larger scale variations in the redistribution process of soil particles.

The empirical semivariogram with the best fitted theoretical model among the Spherical, Gaussian, and Exponential models for each dataset is plotted in Fig. 4. As can be seen, semivariances for all the soil properties from D2 and K_S of D1 reach a plateau, which indicate that the variables in the fields are stationary out of the range. For the properties other than K_S on D1, however, semivariances keep increasing. This suggests that the variables of D1, except for K_S, are more variable than those of D2, because of a longer transportation distance on D1. Normally, the cross-sectional view of the gully shows a V-form, which means that the increase in soil surface elongates the transportation distance for the soil particles. For the silting dam farmland (D2), the shorter transportation distance results in less spatial variability in soil properties. However, the results also suggest that the involved soil properties

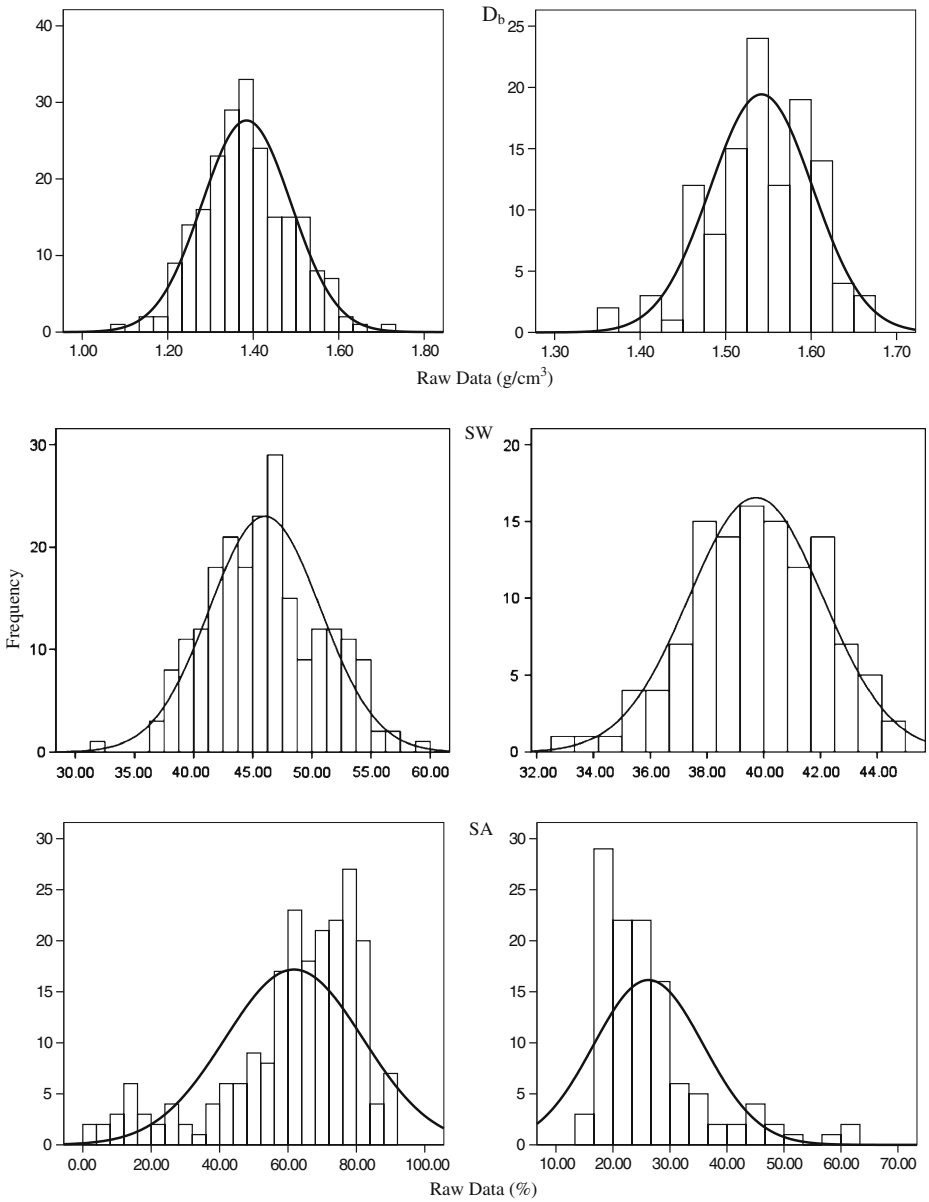

Fig. 3 Histogram of Ks and soil basic physical property. D_b bulk density; SA sand content; SI silt content; CL clay content; SW saturated water content

exhibit spatial dependence within the study area. The existence of spatial patterns in soil parameters at this scale (3 × 3 m) is consistent with the results shown in previous studies (Zeleke and Si 2005).

The nuggets, structural variances, ranges, *GD* values, and best fitted models are presented in Table 2. The fitted model (e.g., Exponential, Gaussian, or Spherical

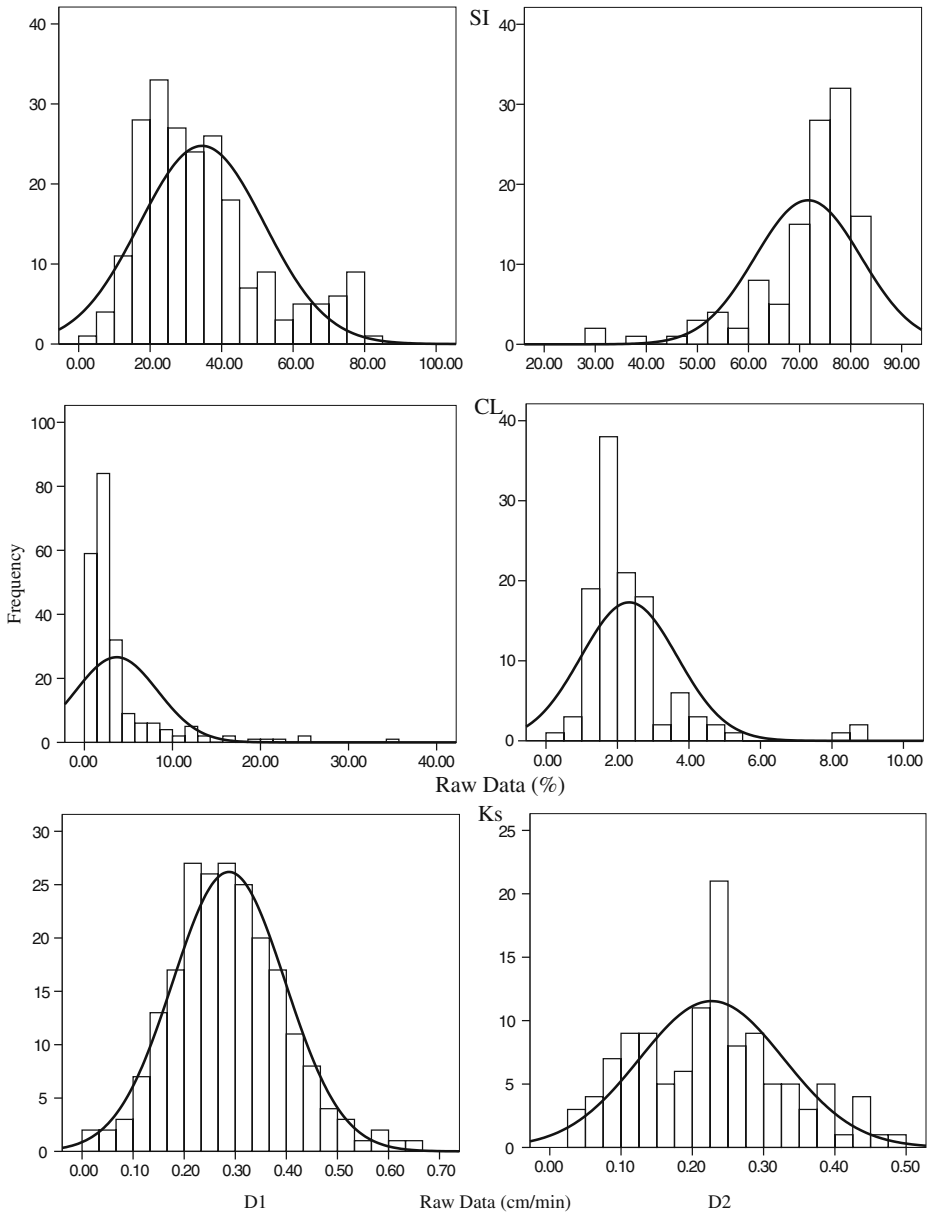

Fig. 3 (continued)

model) with the highest coefficient of determination (R^2) for matching the experimental semivariogram is selected. Except for Ln(CL) of D2 (Exponential model), the same variable on the two dam farmlands has the same model: the semivariograms of D_b, Ln(SA), Ln(SI), and Ln(CL) (only for D1) could be best fitted by the Spherical model, SW by the Gaussian model, and K_S by the Exponential model. The contribution of measurement scale variability to the total variance is estimated

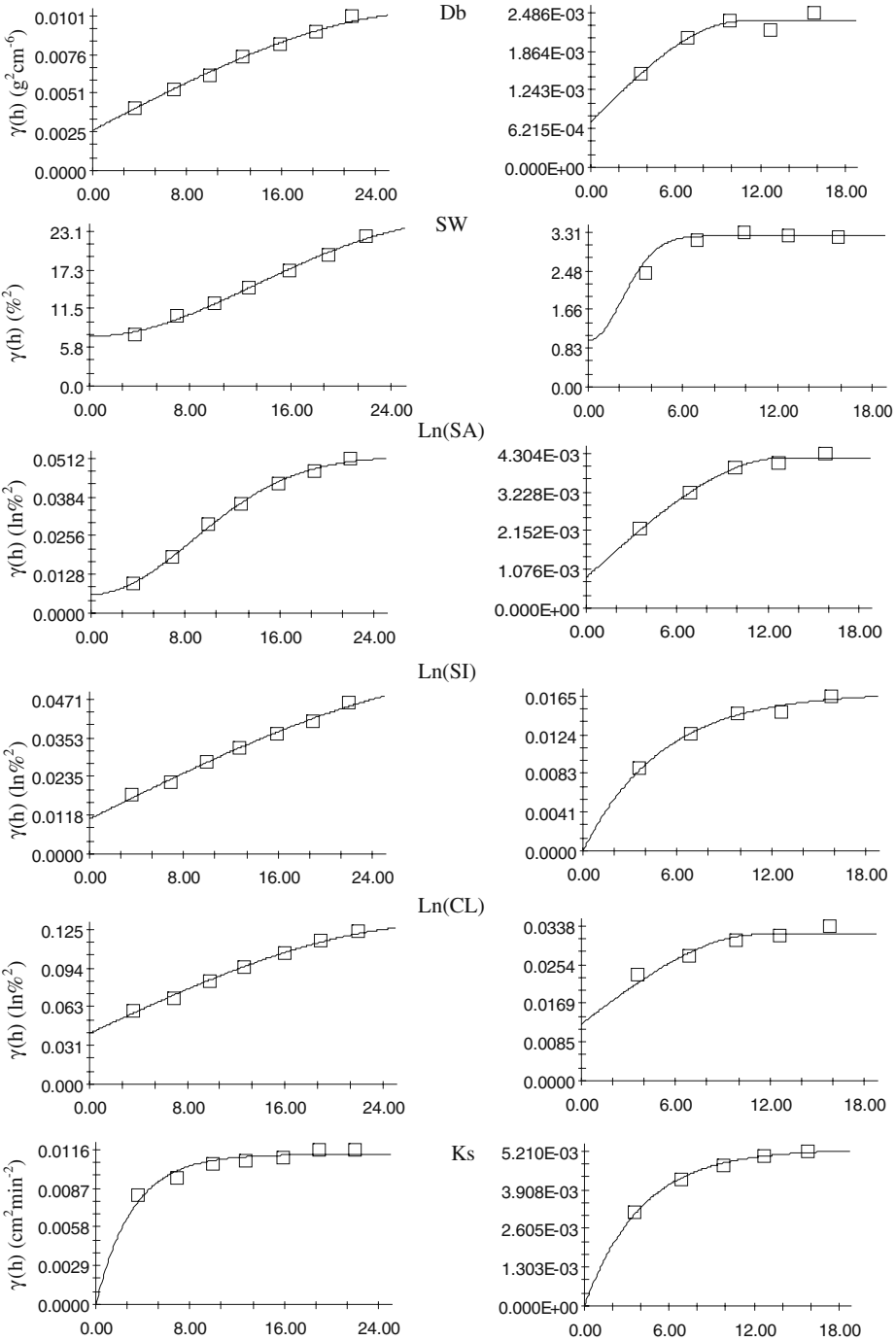
Db
SW
Ln(SA)
Ln(SI)
Ln(CL)
Ks
γ(h) (g²cm⁻⁶)
γ(h) (%²)
γ(h) (ln%²)
γ(h) (ln%²)
γ(h) (ln%²)
γ(h) (cm²min⁻²)
0.0101
0.0076
0.0051
0.0025
0.0000
2.486E-03
1.864E-03
1.243E-03
6.215E-04
0.000E+00
23.1
17.3
11.5
5.8
0.0
3.31
2.48
1.66
0.83
0.00
0.0512
0.0384
0.0256
0.0128
0.0000
4.304E-03
3.228E-03
2.152E-03
1.076E-03
0.000E+00
0.0471
0.0353
0.0235
0.0118
0.0000
0.0165
0.0124
0.0083
0.0041
0.0000
0.125
0.094
0.063
0.031
0.000
0.0338
0.0254
0.0169
0.0085
0.0000
0.0116
0.0087
0.0058
0.0029
0.0000
5.210E-03
3.908E-03
2.605E-03
1.303E-03
0.000E+00
0.00
8.00
16.00
24.00
6.00
12.00
18.00
D1
Lag distance, h(m)
D2

◀ **Fig. 4** Semivariance of soil physical property variables and the natural ln transformed saturated hydraulic conductivity data. *Db* bulk density; *SA* sand content; *SI* silt content; *CL* clay content; *SW* saturated water content; *Ks* saturated hydraulic conductivity

using *GD* values. All the values of *GD* for other variables in Table 2 are <0.75, which indicate that the studied variables do not have a constant variation on the whole scale. The local scale variability in K_S and Ln(SA) is lower than the critical value of 0.25, which is in agreement with the good relationships between K_S and the variable at the 3-m observational scale. Moreover, the low value of *GD* indicates that the spatial heterogeneity caused by structural components plays a major role. The *GD* values derived from the semivariograms indicate the existence of strong spatial dependence for K_S and Ln(SA), and moderate spatial dependence for other variables on the two dam farmlands. From Fig. 4, ranges for the variograms of the variables of D1 are not well defined except for K_S. Within the range, the variables have autocorrelation character. Therefore, the range provides a good measure for the study on similar attribute scopes. Obviously, the variables except for K_S of D1 have larger ranges compared to the ones of D2, and their autocorrelation scopes are also larger and have bigger changes. The ranges of spatial dependency are relatively smaller for Ln(SA), SW, and K_S, especially for D2. The largest range of spatial dependency is found for Ln(SI) of D1 indicating the biggest autocorrelation scope in the variables, followed by D_b of D1.

3.2 Persistency in Spatial Series and Statistical Scale-Invariance

The semivariogram analysis can provide useful information on the magnitude of spatial dependence and the range of spatial dependency. However, for lag distances beyond the range of spatial dependency, the variogram provides only a qualitative description of the variability. For statistically scale-invariant and long range dependent series, quantitative characterization of the variability can be obtained using scal-

Table 2 Summary of the spatial dependence structure of the soil variables on dam farmlands obtained from the best fitted model

	Nugget		Sill		Range (m)		GD		Best fitted model (R^2)	
	D1	D2	D1	D2	D1	D2	D1	D2	D1	D2
D_b	0.0026	0.00073	0.01038	0.0024	29.00	10.71	0.250	0.304	Spherical (0.993)	Spherical (0.928)
Ln(SA)	0.0062	0.00085	0.0519	0.0042	12.23	13.16	0.119	0.202	Spherical (0.990)	Spherical (0.990)
Ln(SI)	0.0107	0.0054	0.0169	0.0164	36.73	15.86	0.633	0.329	Spherical (0.993)	Spherical (0.965)
Ln(CL)	0.0417	0.0124	0.1274	0.0320	28.74	11.37	0.327	0.389	Spherical (0.987)	Exponential (0.921)
SW	7.42	0.987	26.63	3.233	18.48	5.23	0.279	0.305	Gaussian (0.995)	Gaussian (0.978)
Ks	0.00015	0.00001	0.0112	0.00518	11.76	9.02	0.0123	0.002	Exponential (0.892)	Exponential (0.987)

D_b bulk density; *SA* sand content; *SI* silt content; *CL* clay content; *SW* saturated water content; *Ks* saturated hydraulic conductivity

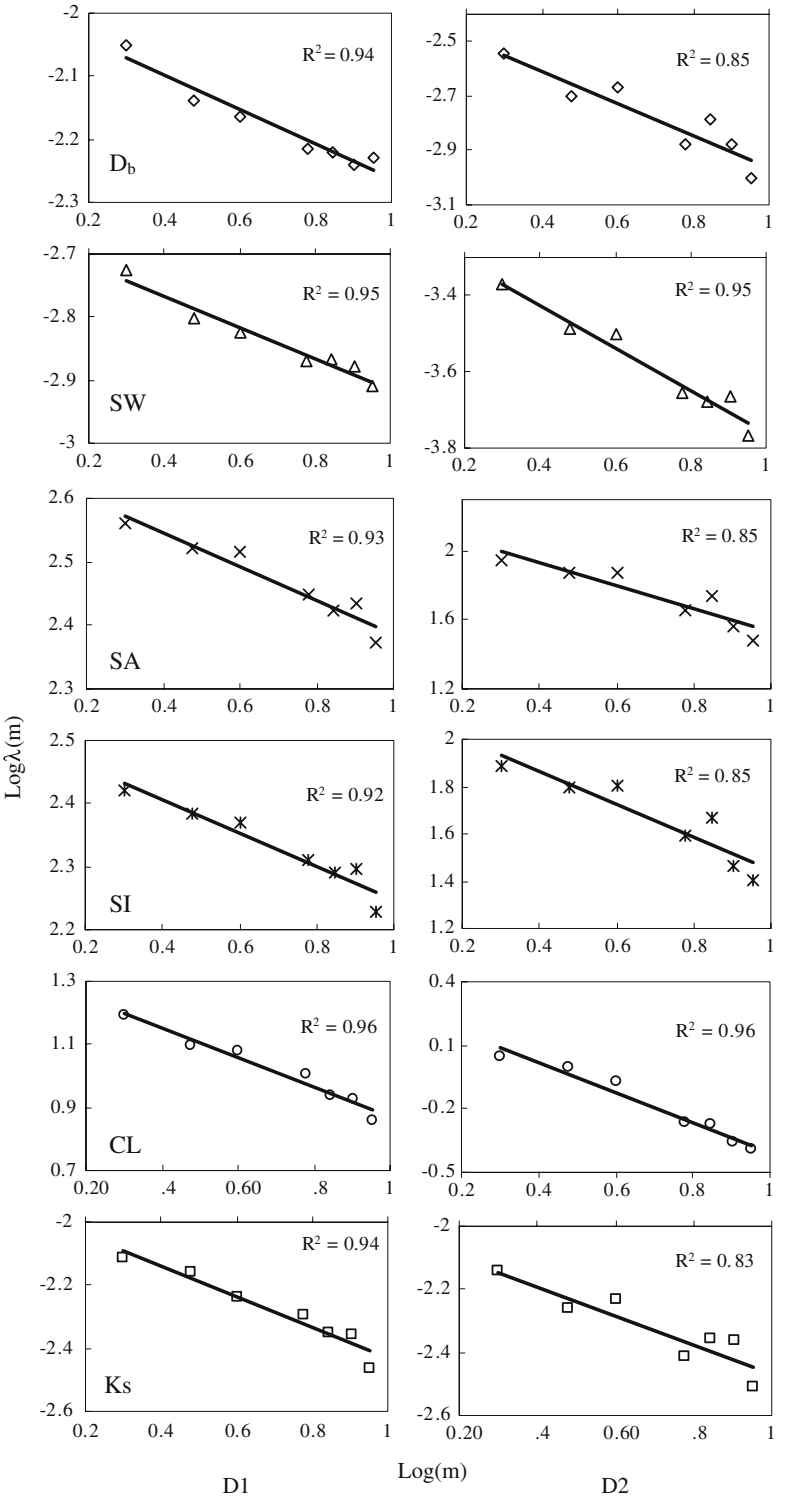
Db
R² = 0.94
R² = 0.85
SW
R² = 0.95
R² = 0.95
SA
R² = 0.93
R² = 0.85
SI
R² = 0.92
R² = 0.85
CL
R² = 0.96
R² = 0.96
Ks
R² = 0.94
R² = 0.83
Logλ(m)
Log(m)
D1
D2

◀ **Fig. 5** Linear fits of the log–log plots of the aggregated variance level of aggregation. D_b bulk density; *SA* sand content; *SI* silt content; *CL* clay content; *SW* saturated water content; *Ks* saturated hydraulic conductivity

ing parameters. To this end, the degree of statistical scale-invariance and persistency in the series are investigated using the log–log plots of the aggregated variance (λ_m) versus the level of the aggregation (m) and the Hurst scaling parameter, H.

The log(λ_m) of all the variables varies linearly with log(m), indicating the presence of statistical scale-invariance (Fig. 5). The coefficients of the determination (R^2) for a linear fit ($n = 7$) for Ks, D_b, SW, SA, SI, and CL are 0.94, 0.94, 0.95, 0.93, 0.92, and 0.96 on D1, respectively, and 0.83, 0.85, 0.95, 0.85, 0.85, and 0.96 on D2 (all significant at $P = 0.01$), respectively. Hence, the degree of statistical self-similarity in the variance structure is the highest for CL, followed by SW on both D1 and D2. The relatively lower R^2 values for Ks, D_b, SA, and SI on D2 indicate a tendency toward more nonlinearity in the log variance versus log scale relationships than the rest of variables on D1 and D2.

The Hurst scaling parameter, H, is determined from the log–log plots of λ_m versus m, and is reported in Table 3. The H values of all the variables on D1 and D2 lie within the theoretical range for a self-similar and long range positively correlated spatial series, say, $0.5 < H < 1.0$. There are, however, slight differences in the H values. Compared to D2, the H values on D1 are slightly higher (but not significant at $P = 0.01$). The slightly higher H values of D1 are possibly because of the uncertainties (the higher R^2 values) in extracting the slope of the log–log plots or higher long-range correlations.

3.3 Spatial Pattern Analysis

The spatial patterns of K_S and soil basic properties interpreted by Kriging methods are plotted in Fig. 6. The distributions of D_b on the dam farmlands are shown in Fig. 6a. Obviously, the highest values of D_b are both found on the silting source of the dam farmlands and the lowest values are found on or near the left bottom of D1 and the top of right corner on D2, where both locations are relatively far away from the silting source of the dam farmland. Generally, D_b is closely related to soil textures (Zeleke and Si 2005). Therefore, we speculate that this phenomenon is strongly related to the particle redistribution processes on the dam farmlands. The distributions of SW on the two dam farmlands are shown in Fig. 6b. The dam farmlands could be more easily saturated by the collected runoff. Moreover, the saturated surface soil layers are related to the runoff generation. It can be seen

Table 3 The Hurst scaling parameter values

	H	
	D1	D2
Ks	0.863 (0.024)	0.705 (0.066)
D_b	0.867 (0.025)	0.665 (0.051)
SW	0.868 (0.021)	0.652 (0.016)
SA	0.764 (0.031)	0.646 (0.049)
SI	0.877 (0.033)	0.719 (0.048)
CL	0.754 (0.014)	0.770 (0.013)

D_b bulk density; *SA* sand content; *SI* silt content; *CL* clay content; *SW* saturated water content; *Ks* saturated hydraulic conductivity

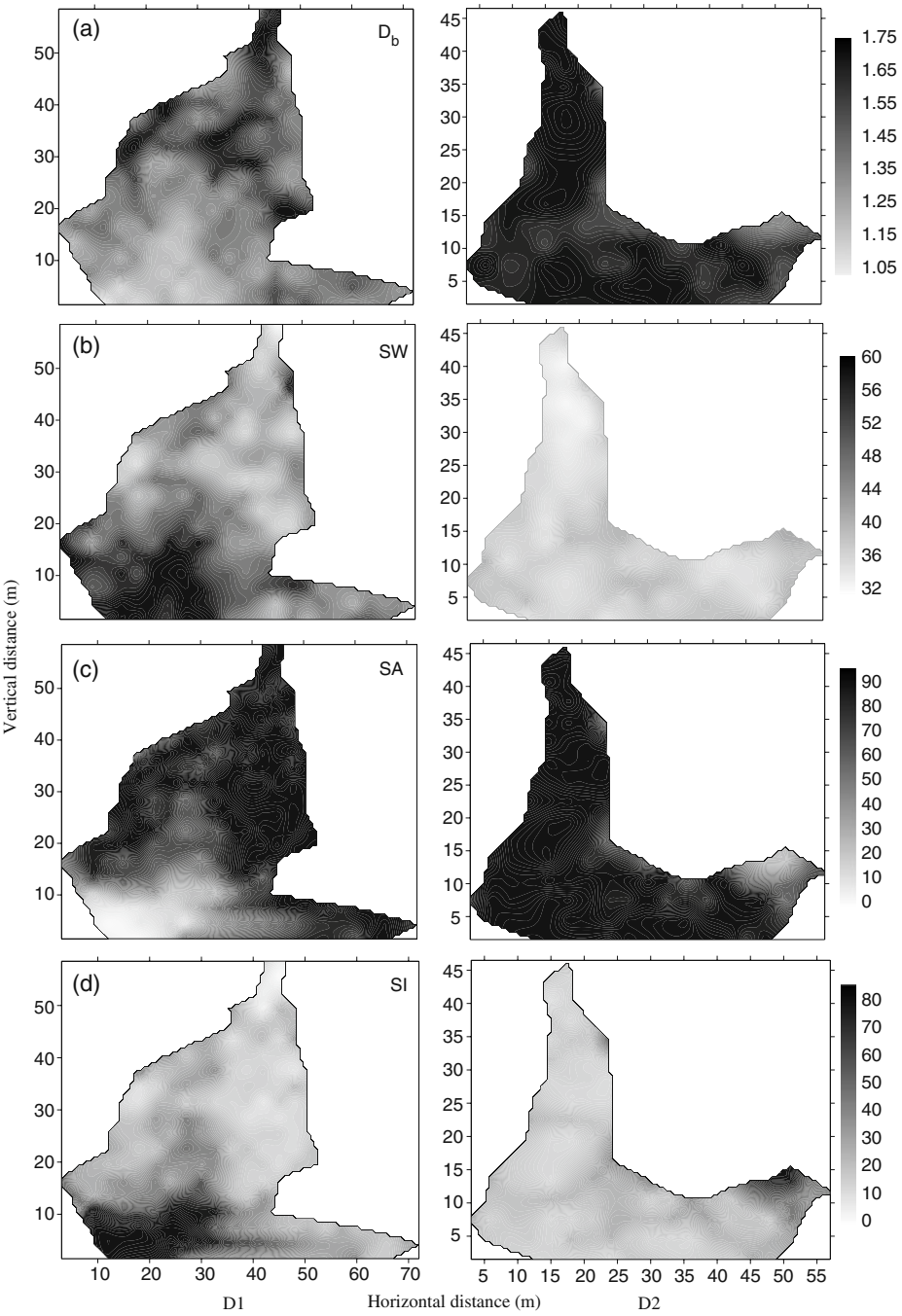

Fig. 6 The spatial distribution of Ks and soil basic properties

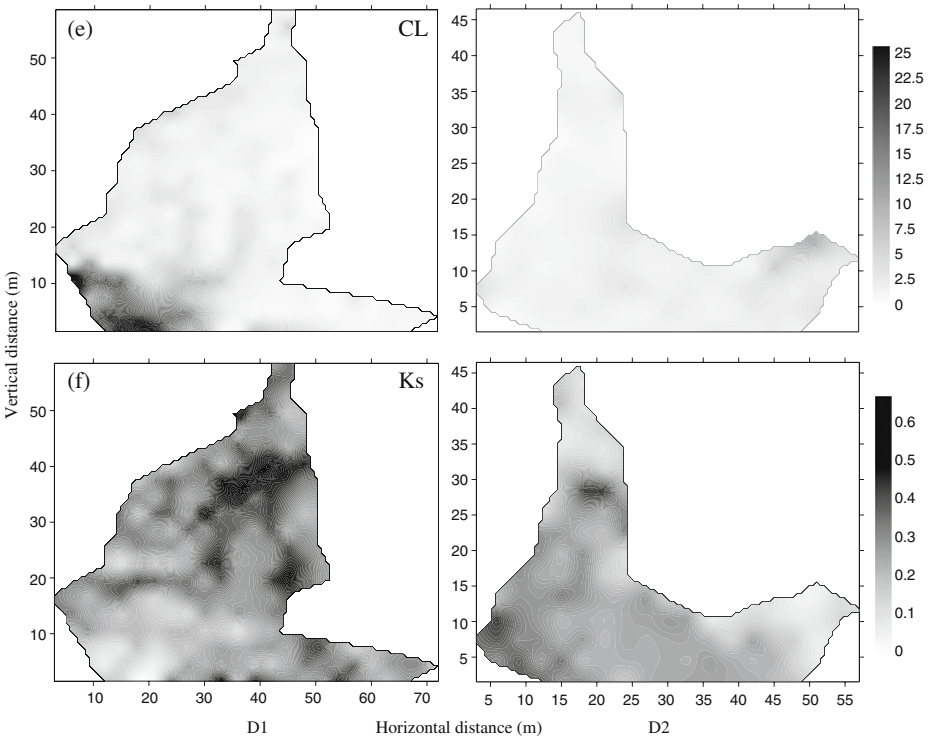

Fig. 6 (continued)

from Fig. 6b that the spatial distributions of SW do not exhibit greater difference compared to the ones of D_b. The high values of SW are found on or near the left bottom of D1 and on the top of the right corner of D2, which are the same locations where the lowest values of D_b are found. The spatial patterns of the SA, SI, and CL fractions on the dam farmlands are shown in Fig. 6c, d, e, respectively. On D1, the contents of SI and CL increase from the silting source to the bottom of the dam farmland, while the content of SA decreases. On D2, the spatial patterns of the distributions of the SA, SI, and CL fractions are not as clear as those observed on D1. Generally, high SA contents are found on the silting source of D2; whereas, high SI and CL contents are concentrated on the top of the right corner of D2, where surface runoff can not reach easily. However, this finding contrasts with the results of Ampontuah et al. (2006), who found that the contents of clay and fine silt decrease from upslope to downslope due to the preferential detachment of coarser particles. The spatial distribution patterns observed in this study is mainly because that the coarser sediments carried by the surface runoff would first deposit on the source of the dam farmland. It is well established that the sediment transport capability of surface runoff dominates the sediment redistribution processes in fluvial plains, and larger soil particles would deposit first and finer particles would be transported further distance (Young 1980). This well explains the redistribution of the SA, SI, and CL fractions on D1. The low contents of CL (Fig. 6e) at the site are primarily because sandy loam soils are dominant (Hu et al. 2008) and stability in the soil

erosion process (Young 1980). As a consequence, the spatial distributions of D_b and SW correspond to the sediment redistribution processes with larger D_b values corresponding to higher SA contents and larger SW values corresponding to higher SI contents.

The spatial distributions of K_S on the two undisturbed dam farmlands are shown in Fig. 6f. It is apparent that the highest K_S values are found on the middle part of the dam farmlands, while the lowest K_S values are found on or near the left bottom on D1 and on the top of the right side corner of D2, where both locations are further way from the sources of the dam farmland. The lowest K_S values are found on the same locations where had the lowest values of D_b and SA and the highest values of SI, CL and SW. However, the locations, where the highest K_S values are observed, are different with the zones of the highest values of D_b and SA and the lowest values of SI, CL fractions, and SW. This could be explained by that besides the soil intrinsic properties, the activities of soil fauna also could affect the K_S in the topsoils. During the field campaign, we also observed that the activities of soil fauna are very active on the middle part of the dam farmlands. Affected by the frequent silting processes and elevated soil surfaces due to the sedimentation process, very few animals are found on the silting source of the dam farmlands, where the highest values of D_b and SA contents are observed. Even if the soil fauna could disturb the soil structure, the frequent silting processes also can cover the previous surface soil layers. Different from the silting sources, vegetations are mostly located in the middle portion for the sufficient sunlight and relatively loose soil structures. Consequently, the soil fauna was like to live in the middle part of dam farmland for sufficient sunlight and relatively stable inhabits (less erosion). The activities of soil fauna might disturb the soil structure and result in higher K_S values (Mishra et al. 2007). In addition, compared to the silting sources, there are less silting processes occurring on the middle part of the dam farmlands due to a longer transportation distance. Although the area with the highest K_S value dose not exactly correspond to the one with the highest D_b values and SA contents, the locations where the highest K_S occurs also have very high SA contents and D_b values, suggesting that coarser particles are crucial in controlling K_S. Blanco-Canqui et al. (2002) also reported that sand soils typically result in high K_S values.

Figure 7 shows the linear relationships among D_b, SW, SA, and SI with K_S. The degree of correlation between K_S and the soil physical properties at the observational scale are evaluated using Pearson's correlation coefficient as listed in Table 4. K_S is correlated with all the soil basic properties on both D1 and D2 (significant at $P = 0.01; n = 216$ on D1 and 120 on D2). It is apparent that at this scale (i.e., the 3-m observation interval) the spatial variability in K_S is mainly explained by the trade-off between SA and SI contents and other factors that determine the distribution of macropores. The similarity in local scale variability between K_S and SA is also in agreement with the significant relationships between the two variables as observed from the GD values (both <0.25). The significant correlation between K_S and SA at this scale is in agreement with the observation by Zeleke and Si (2005). In general, the SA fraction is mostly correlated with K_S the on dam farmlands with the largest coefficient of correlation (Table 4 and Fig. 7). The SW, SI, and CL

Fig. 7 The linear relationship among Ks and soil basic properties ▶

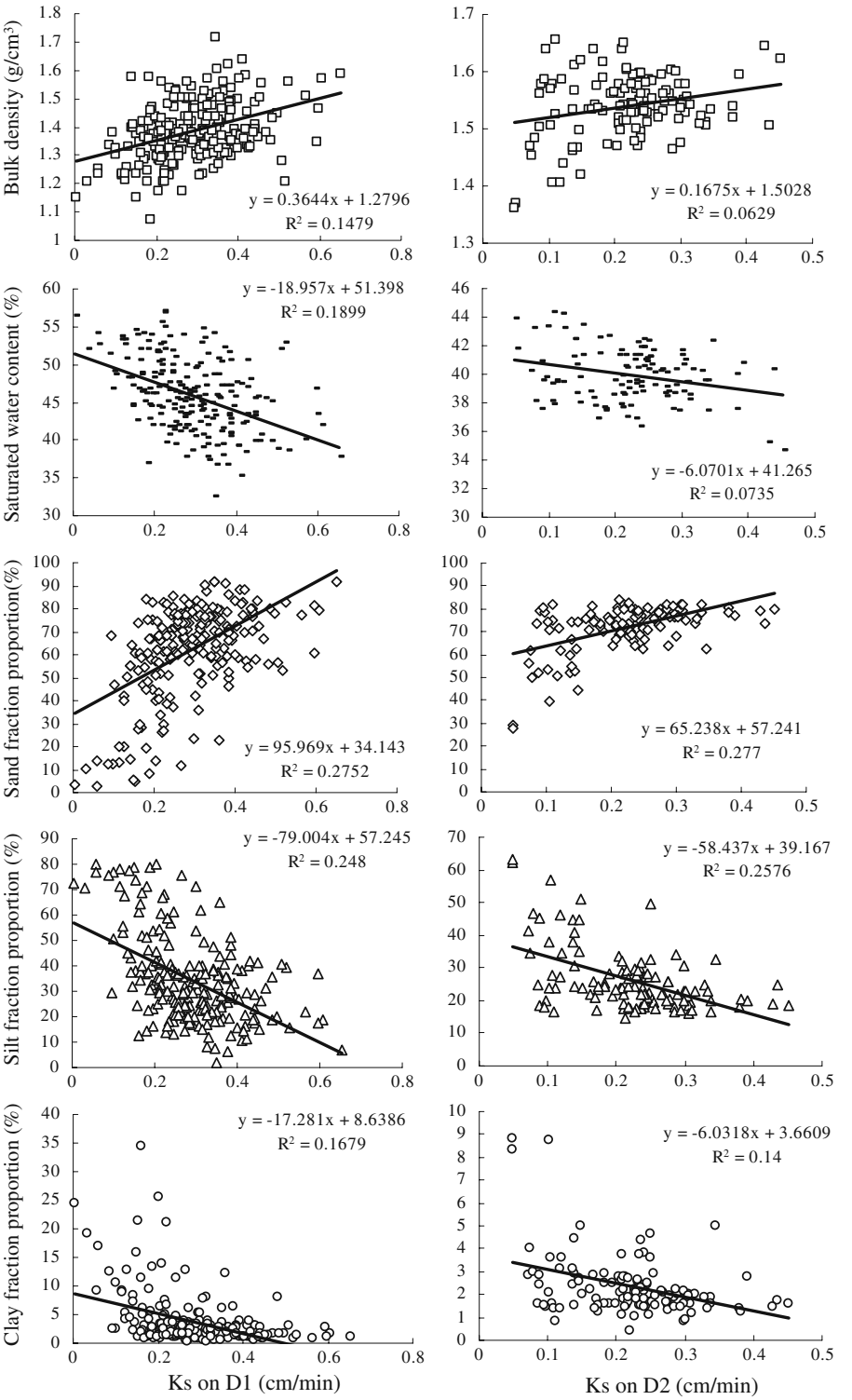
Bulk density (g/cm³)
y = 0.3644x + 1.2796
R² = 0.1479
y = 0.1675x + 1.5028
R² = 0.0629
Saturated water content (%)
y = -18.957x + 51.398
R² = 0.1899
y = -6.0701x + 41.265
R² = 0.0735
Sand fraction proportion(%)
y = 95.969x + 34.143
R² = 0.2752
y = 65.238x + 57.241
R² = 0.277
Silt fraction proportion (%)
y = -79.004x + 57.245
R² = 0.248
y = -58.437x + 39.167
R² = 0.2576
Clay fraction proportion (%)
y = -17.281x + 8.6386
R² = 0.1679
y = -6.0318x + 3.6609
R² = 0.14
Ks on D1 (cm/min)
Ks on D2 (cm/min)

Table 4 Pearson's correlation analysis between *Ks* and the variables

	Ks	D_b	SW	SA	SI
D1					
D_b	0.385[a]	1			
SW	−0.436[a]	−0.874[a]	1		
SA	0.525[a]	0.714[a]	−0.749[a]	1	
SI	−0.498[a]	−0.695[a]	0.730[a]	−0.979[a]	1
CL	−0.410[a]	−0.462[a]	0.494[a]	−0.648[a]	0.484[a]
D2					
D_b	0.251[a]	1			
SW	−0.271[a]	−0.509[a]	1		
SA	0.526[a]	0.777[a]	−0.480[a]	1	
SI	−0.508[a]	−0.763[a]	0.474[a]	−0.978[a]	1
CL	−0.374[a]	−0.569[a]	0.340[a]	−0.755[a]	0.689[a]

[a]Correlation is significant at the 0.01 level (two-tailed)
D_b bulk density; *SA* sand content; *SI* silt content; *CL* clay content; *SW* saturated water content; *Ks* saturated hydraulic conductivity

contents are negatively correlated with K_S, while SA and D_b are positively correlated to K_S.

4 Conclusions

In this study, we investigated the spatial pattern of near-surface K_S at two dam farmlands located in the Loess Plateau of China. The semivariograms for different soil parameters reveal that the soil property fields are more stationary at the silting dam farmland than the filled one in a limited range. Less variability of soil properties was more suitable to precision agriculture. Analysis using Pearson correlation coefficients showed that the spatial variation in K_S (at the observation scale) was significantly correlated with the spatial distributions of soil texture, saturated water content (SW), and bulk density (D_b) at both filled dam farmland (D1) and silting dam farmland (D2) under natural silting conditions. The values of scaling parameter (H) for all soil parameters at D1 and D2 lie within the theoretical range for a self-similar and long range positively correlated spatial series. The areas with lowest K_S values corresponded to the areas with the highest CL, SI, and SW, indicating that the uplands of the dam farmlands are more prone to surface runoff. The area with the highest K_S value was found at the middle portion of the dam farmlands with relative higher SA and D_b values (not the highest) which can benefit floodwater and runoff control. The implication of scale dependent variability is that small-scale descriptions of K_S may not be sufficient to fully describe the relationship between K_S and soil properties. Hence, future research in improving mutifractal methods as well as K_S interpolation techniques should incorporate several spatial scales during the modelling and validation process. It is also well established that the farming activities can disturb soil structure and increase water infiltration. Therefore, we suggest planting crops such as maize (*Zea mays* L.) at dam farmlands for the purposes of floodwater control, crop yield, and mitigation of floods.

Acknowledgements Financial support was given by the CAS/SAFEA, International Partnership Program for Creative Research Teams—Process simulation of soil and water of a watershed and

Program for Innovative Research Team in University (No. IRT0749). The authors thank the reviewers for the English review and critical comments.

References

Ampontuah EO, Robinson JS, Nortcliff S (2006) Assessment of soil particle redistribution on two contrasting cultivated hillslopes. Geoderma 132:324–343

Blanco-Canqui H, Gantzer CJ, Anderson SH, Alberts EE, Ghidey F (2002) Saturated hydraulic conductivity and its impact on simulated runoff for Claypan Soils. Soil Sci Soc Am J 66:1596–1602

Braun P, Molnar T, Kleeberg HB (1997) The problemofscaling in grid-related hydrological process modeling. Hydrol Process 11:1219–1230

Burt TP (2001) Integrated management of sensitive catchment systems. Catena 42:275–290

Cambardella C, Mooman TB, Novak JM, Parkin TB, Karlem DL, Turvo RF, Konopa AE (1994) Field scale variability of soil properties in central lowa soil. Soil Sci Soc Am J 47:1501–1511

Chen YZ, Luck SH (1989) Sediment sources and recent changes in the sediment load of Yellow River, China. In: Rindwanich S (ed) Land conservation for future generations. Ministry of Agriculture, Bangkok, pp 313–323

De Vries JJ, Simmers I (2002) Groundwater recharge: an overview of processes and challenges. Hydrogeol J 10:5–17

Gao ZL, Zhang XP (2007) Study on the construction and layout of check-dam in the Loess Plateau. The Literature Publisher, Beijing (in Chinese)

Grego CR, Vieira SR, Antinio AM, Rosa SCD (2006) Geostatistical analysis for soil moisture content under no tillage cropping system. Sci Agr 63:341–350

Hu W, Shao MA, Wang QJ, Fan J, Reichardt K (2008) Spatial variability of soil hydraulic properties on a steep slope in the Loess Plateau of China. Sci Agr 65:268–276

Kettler TA, Doran JW, Gilbert TL (2001) Simplified method for soil Particle—size determination to accompany soil quality analysis. Soil Sci Soc Am J 65:849–852

Lee CK (2002) Multifractal characteristics in air pollutant concentration time series. Water Air Soil Pollut 135:389–409

Massey FJ (1951) The Kolmogorov–Smirnov test of goodness of fit. J Am Stat Assoc 46:1–70

Mishra A, Kar S, Singh V (2007) Prioritizing structural management by quantifying the effect of land use and land cover on watershed runoff and sediment yield. Water Resour Manage 21: 1899–1913

Nielsen DR, Bouma J (1985) Soil spatial variability. PUDOC, Wageningen, pp 2–30

Pardini G (2003) Fractal scaling of surface roughness in artificially weathered smectite-rich soil regoliths. Geoderma 117:157–167

Rai SN, Ramana DV, Singh RN (1998) On the prediction of ground-water mound formation in response to transient recharge from a circular basin. Water Resour Manage 12:271–284

Shi H, Shao M (2000) Soil and water loss from the Loess Plateau in China. J Arid Environ 45:9–20

Sobieraj J, Elsenbeer H, Cameron G (2004) Scale dependency in spatial patterns of saturated hydraulic conductivity. Catena 55:49–77

Tabachnick BG, Fidell LS (1996) Using multivariate statistics, 3rd edn. Harper Collins, New York

Tang KL, Hou QC, Wang BK, Zhang PC (1993) The environment background and administration way of Wind-Water Erosion Crisscross Region and Shenmu experimental area on the Loess Plateau. Memoir of NISWC, Academia Sinica and MWR 18:2-15 (in Chinese)

Teverovsky V, Taqqu M (1997) Testing for long-range dependence in the presence of shifting means or a slowly declining trend, using a variance-type estimator. J Time Ser Anal 18:279–304

Wang T, Istanbulluoglu E, Lenters J, Scott D (2009a) On the role of groundwater and soil texture in the regional water balance: an investigation of the Nebraska Sand Hills, USA. Water Resour Res 45, W10413, doi:10.1029/2009WR007733

Wang T, Zlotnik V, Šimunek J, Schaap M (2009b) Using pedotransfer functions in vadose zone models for estimating groundwater recharge in semiarid regions. Water Resour Res 45:W04412, doi:10.1029/2008WR006903

Wang T, Wedin D, Zlotnik V (2009c) Field evidence of a negative correlation between saturated hydraulic conductivity and soil carbon in a sandy soil. Water Resour Res 45, W07503, doi:10.1029/2008WR006865

Xu M, Wang G (2000) To accelerate the construction of check-dams in the Loess Plateau. Yellow River 22:26 (in Chinese)
Young RA (1980) Characteristics of eroded sediment. Trans ASAE 23:1139–1142, 1146
Zeleke TB, Si BC (2005) Scaling relationships between saturated hydraulic conductivity and soil physical properties. Soil Sci Soc Am J 69:1691–1702
Zhang HJ, Yan JP, Zhou LH (2007) The influence of Loess Plateau soil-saving dam on water resources: An example of typical soil-saving dam of Jiuyuangou in suide county. Journal of Northwest University (Natural Science Edition) 37:475–478 (in Chinese with English abstract)
Zhou X, Persaud N, Wang H (2004) Periodicities and scaling parameters of daily rainfall over semi-arid Botswana. Ecol Model 182:371–378